Large plasmonic resonance shifts from metal loss in slits

Zohreh Sharifi · Reuven Gordon*

Received: date / Accepted: date

Abstract The impact of loss on the plasmonic resonances in metal-insulator-metal slits is analyzed, particularly the significant effect of loss on the reflection phase. The reflection is calculated analytically using single mode matching theory with the unconjugated form of the orthogonality relation. This theoretical calculation agrees well with comprehensive simulations, but differs substantially from the conjugated orthogonality result, as was used in past analytical works. This reflection phase has a large impact on the plasmonic resonance wavelengths, which are calculated using a Fabry-Pérot theory and compared with past experiment and finite-difference time-domain simulations.

Keywords Plasmonic resonances · Plasmonic gaps · Slit in a real metal

1 Introduction

Subwavelength slits in metal allow for confining light to the nanometer scale [1–4], which is a million times smaller than the wavelength for millimeter waves [5,6]. While the non-resonant case already supports 10^4 field enhancement [7], the resonant case gives even larger enhancement by constructive interference with multiple reflections from the end faces of the slit [8–11]. Metal-insulator-metal (MIM) plasmonic slits also enhance optical absorption [12,13]. There has also been great interest in analyzing the dispersion properties of MIM structures[14–16]. The easy fabrication of the MIM structures makes this geometry well-suited for nanophotonic applications [17–21].

R. Gordon (*corresponding author)
Department of Electrical and Computer Engineering, University of Victoria, Victoria, British Columbia, Canada V8W 3P6
E-mail: rgordon@uvic.ca

Z. Sharifi
Department of Electrical and Computer Engineering, University of Victoria, Victoria, British Columbia, Canada V8W 3P6

The theory of the transmission of light through single slit in a perfect electric conductor has been studied extensively in the past [22,23]. It was shown that the maxima in the transmission spectrum are different from the normal Fabry-Pérot resonances, with zero phase shift upon reflection, as confirmed by experiment [24]. In MIM structures, the plasmon wavevector and the phase of reflection from the end faces determines the resonant length of the cavity. The resonance length is not equal to the simple multiple of the half-wavelength in general because of large reflection phase [25,26]. Therefore, to predict MIM cavity resonances, calculation of the reflection phase is necessary.

SPP reflection has been investigated for single slit with different dielectric and metallic materials [27–29]. For MIM cavities, analytical calculations of the reflection phase have been done for lossless and dispersion-free metals by our group [23]. Another group advanced this theory for a real metal while still using the conjugated form of the orthogonality relation [30].

In this paper, we calculate analytically the reflection coefficient and phase acquired by SPPs upon reflection from the slit end-face using a simple mode matching model for real metals exhibiting both dispersion and loss. The approach is similar to past works [23,30] except that we employ the unconjugated form of the orthogonality relation. Our method shows good agreement with comprehensive finite difference time domain (FDTD) simulations, even for thin slits at the nanometer scale. By comparison, we show that the conjugated form of the orthogonality, as used in past works, differs considerably from the simulation results at shorter wavelengths, especially for narrower slits. We use the reflection phase to calculate plasmon resonances and plot the dispersion. The resulting dispersion shows good agreement with past experimental results [1]. The unconjugated approach is more accurate than the conjugated form because the conjugated form is not a proper orthogonality relation (i.e., it gives non-zero values for different modes) when there is loss or gain [31] The unconjugated form is a proper orthogonality relation for the loss/gain cases and it isolates each mode given a value of zero for different modes — for the case of single mode matching approximation, the unconjugated form is therefore more accurate. It is possible to calculate the phase for non-resonant cases. We attempted this approach to calculate the phase [32], however we found that it is numerically challenging and does not give a clear physical interpretation. Our theory shows a clear physical peak that makes the analysis more transparent.

2 Unconjugated orthogonality reflection theory

Fig. 1 shows a schematic of the MIM waveguide resonator. Two infinitely thick metal layers are separated by a thin dielectric. The thickness of the dielectric is denoted by w and the SPPs propagate in the z direction. The metal permittivity and the insulator (dielectric) permittivity are ϵ_m and ϵ_d.

Loss affects the cavity resonance by changing the phase of reflection, in addition to the quality factor. In general, MIM waveguides support SPP modes with both symmetric and antisymmetric electric field profiles. If the dielectric

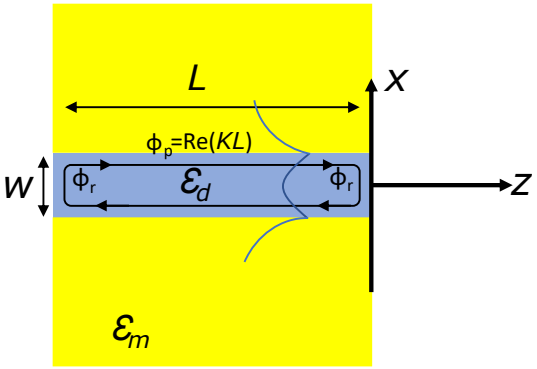

Fig. 1 Schematic representation of the slit with complex permittivity ϵ_d in a real metal with complex permittivity ϵ_m. The electric field profile of the symmetric SPP mode is shown.

is sufficiently thin, only the mode with a symmetric field profile is propagating; such cavities are considered here. We calculate the propagation constant and the reflection coefficient at the interface to free space for the fundamental TM mode within a slit.

The spatial dependence of the x component of the electric field for the lowest order TM mode within the slit can be formulated as:

$$E_x^s(x,z) = \begin{cases} \cosh\left(\sqrt{\varepsilon_d k_0^2 - k_z^2}\,x\right)\exp\left(ik_z z\right) & \text{if} |x| \leqslant w/2 \\ \frac{1}{\varepsilon_m}\cosh\left(\sqrt{\varepsilon_d k_0^2 - k_z^2}\,\frac{w}{2}\right) f\left(k_z,x\right)\exp\left(ik_z z\right) & \text{if} |x| > w/2 \end{cases} \quad (1)$$

,

$$f\left(k_z,x\right) = \exp\left[-\sqrt{k_z^2 - \varepsilon_m k_0^2}(|x| - w/2)\right]$$

where the superscript s denotes the MIM surface plasmon electric field, k_z is the propagation constant in the z direction, k_0 is the free-space wave vector. The corresponding y component of the magnetic field can be found using the Maxwell-Ampère relation.

The propagation constant is given by:

$$\tanh\left(\sqrt{k_z^2 - \epsilon_d k_0^2}\,w/2\right) = \frac{-\epsilon_d\sqrt{k_z^2 - \epsilon_m k_0^2}}{\epsilon_m\sqrt{k_z^2 - \epsilon_d k_0^2}}. \quad (2)$$

We solve this equation for complex k_z by an iterative approach.

The reflection coefficient is calculated using single mode matching theory with the unconjugated orthogonality. Continuity of the tangential electric and magnetic fields at the boundary, z=0, gives:

$$(1+r)E_x^s = \int_{-\infty}^{\infty} t\left(k_x\right)\exp\left(ik_x x\right)dk_x \quad (3)$$

$$(1-r)H_y^s = \int_{-\infty}^{\infty} \frac{t\,(k_x)\,\omega\varepsilon_0}{\sqrt{k_0^2-k_x^2}} \exp\left(ik_x x\right) dk_x \tag{4}$$

where the electric field in the free space region is written as an infinite sum of plane wave modes and t and r are transmission and reflection coefficients.

Using the unconjugated form of the orthogonality relation we multiply both side of Equation 3 and 4 by H_y^{fs} and E_x^s, where H_y^{fs} which is the free space magnetic field equals

$$H_y^{fs} = \int_{-\infty}^{\infty} \exp\left(ik_x' x\right) dx \tag{5}$$

where k_x' is the free space plane wave propagation constant. Then Equations 3 and 4 convert to

$$\int_{-\infty}^{\infty} (1+r) e^{ik_x' x} E_x^s dx = \int_{-\infty}^{\infty} t\,(k_x) \exp\left(\left(ik_x + ik_x'\right) x\right) dk_x \tag{6}$$

$$\int_{-\infty}^{\infty} (1-r) \frac{\omega\varepsilon}{\beta} \left(E_x^s\right)^2 dx = \omega\varepsilon_0 \int_{-\infty}^{\infty} \frac{t\,(k_x)}{\sqrt{k_0^2-k_x^2}} \left[\int_{-\infty}^{\infty} E_x^s \exp\left(ik_x x\right)\right] dk_x \tag{7}$$

solving Equations 6 and 7 for r, the reflection coefficient can be found:

$$r = \frac{1-G}{1+G} \quad , \quad G = \frac{1}{2\pi} \frac{\int_{-\infty}^{\infty} \frac{k_0}{Z_0\sqrt{k_0^2-k_x^2}} \left[\int_{-\infty}^{\infty} E_x^s \exp\left(ik_x x\right)\right]^2 dk_x}{\int_{-\infty}^{\infty} E_x^s(x,0) H_y^s(x,0) dx} \tag{8}$$

where H_y^s is the surface plasmon magnetic field in the cavity, Z_0 is the characteristic impedance of free space. We calculate k_z from Equation 2 for lossy and lossless cases (with and without considering the imaginary part of the relative permitivity of the metal) and use the values to calculate the elctric and magnetic field using Equation 1 and then calculate the reflection coefficient in Eqution 8. Comparing Equation 8 with past work [30], the unconjugated orthogonality is different here and appears in the denominator of G. This has a significant impact on the reflection coefficient when loss is considered.

Fig. 2 shows the impact of loss for an Au-air-Au structure. As it is clear for shorter wavelengths and shorter width, the metal loss affects phase of reflection. In a lossy MIM structure, the mode index does not get as large as in the lossless case at short wavelengths. Consequently, the smaller index and the decreased confinement lead to the difference for lossy and lossless case. At longer wavelengths, because the SPP mode is pushed out of the metal, losses are negligible and the reflection characteristics are similar to the lossless case. A huge difference can also be seen when considering the unconjugated form of the orthogonality relation. To make a comparison with past work [30], the phase of reflection has been calculated for three different metals (Au,Al,Ag). Fig. 3 compares phase of reflection for slit width of 50 nm considering loss of the metal using both conjugated and unconjugated forms. Comparing the results for Ag with the results past works [30], the difference of reflection phase in the

two methods is obvious. This shows the importance of considering both the metal loss and conjugated form of the orthogonality relation in the calculation of the reflection phase.

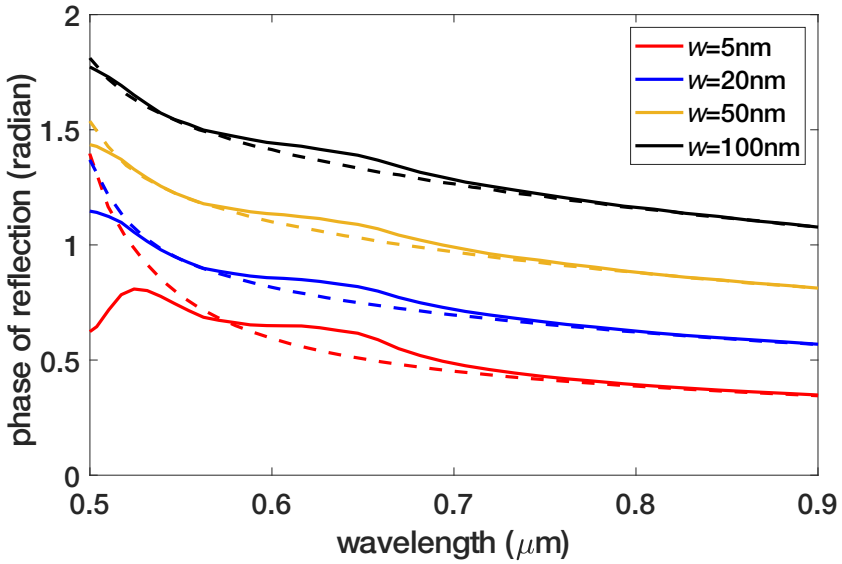

Fig. 2 Reflection phase for an Au-air-Au structure as a function of wavelength for different slit width. Solid lines show the results for the lossy cases and dashed lines show the results for the lossless cases.

Fig. 4 compares reflection coefficient phase for an Au-air-AU structure for different slit width using both the conjugated [30] and unconjugated forms of the orthogonality. The unconjugated form results are plotted with solid lines and the conjugated results are plotted with dashed lines. A clear and significant difference is seen between the two approaches, which is most profound for narrower slits and shorter wavelengths. The reflection phase decreases with increasing wavelength and is larger for a thicker slit. The phase is clearly affected by the introduction of losses in the metal, which is different from what was suggested in past works [30].

3 Comparison with FDTD simulations

To determine the validity of this theory, we used commercial FDTD simulations (Lumerical FDTD ver. 2020 R2.3). Perfectly matched layer boundary conditions were used to prevent reflection of the outgoing waves. The simulation cross-section area was chosen to surround the whole structure. The mesh sizes along the x and z directions were reduced in size to ensure convergence (which was achieved at 0.01 nm for the smallest slit). A normally incident plane wave source was used to excite the structure. The simulation domain

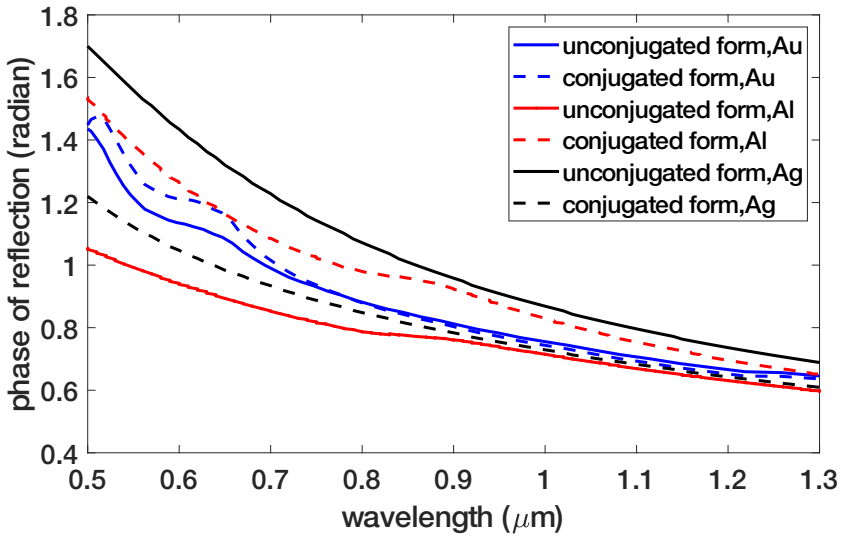

Fig. 3 Reflection phase as a function of wavelength for a MIM structure for different metals and using the conjugated and unconjugated form of the orthogonality relation for slit width of 50 nm.

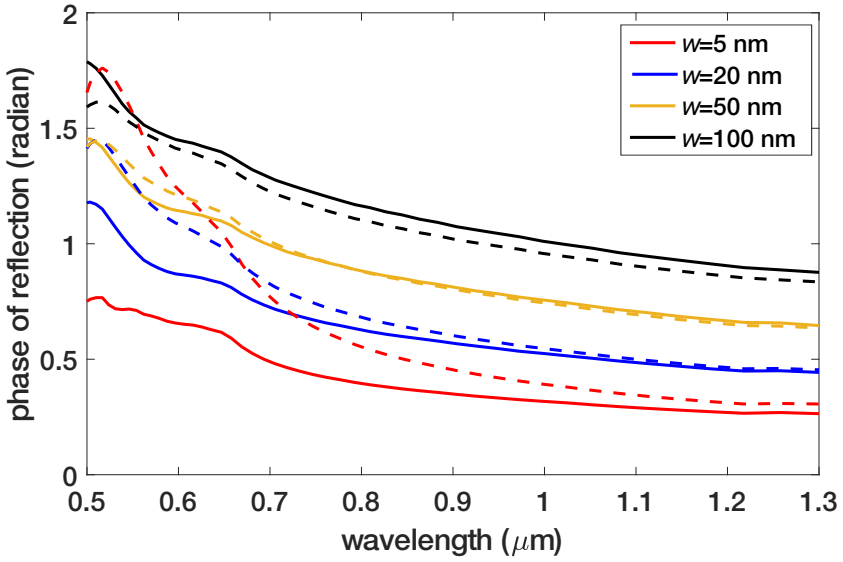

Fig. 4 Reflection phase for an Au-air-Au structure as a function of wavelength for different slit width. Solid lines show the results using unconjugated form of the orthogonality and dashed lines show the results using the conjugated form of the orthogonality.

was 1.6×1.5 μm. A frequency domain power monitor was placed at the exit side of the slit to record the transmission. In addition to convergence tests, the simulations were compared with past simulations for the same conditions.

Fig. 5 shows the power distribution inside the slit for the slit width of 20 nm and L=250 nm. A TM-polarized plane wave of λ=1.08 μm is incident from the left. The white dashed lines are the borders of the slit.

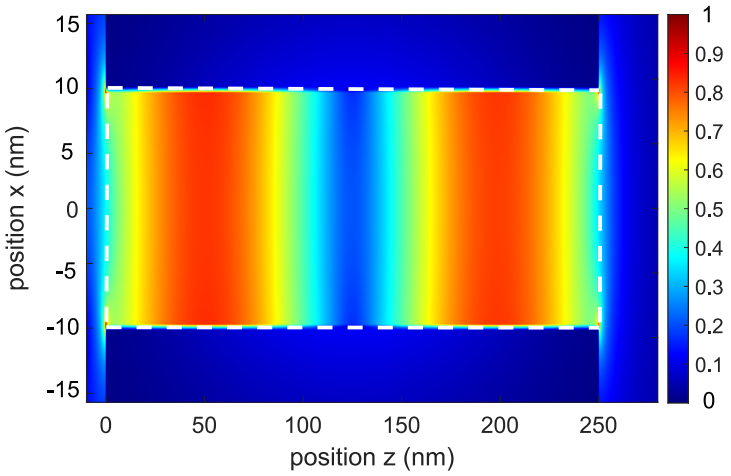

Fig. 5 Power distribution inside the slit for the slit width of 20 nm and L=250 nm. A TM-polarized plane wave of λ=1.08 μm is incident from the left. The white dashed lines are the borders of the slit.

Fig. 6 a and b shows the electric and magnetic fields inside the structure along the z and x directions. The figure compares well with past simulations [20]. Energy confinement is clearly visualized in the Figures. Furthermore, the field distribution shows a standing wave inside the MIM region. Note that the electric field is maximized near the entrance and the exit surfaces. The strong energy confinement of MIM cavities can give strong light-matter interaction, even with losses considered.

Fig. 7 shows the numerically simulated transmission through slit width of 20 nm for different values of L. Resonant transmission peaks are observed with a wavelength that increases as the slit length increases. The propagation constant, k_z, at the resonance wavelength was calculated in FDTD using the mode-source feature. The phase of reflection, Φ_r, was calculated using

$$\Phi_r = m\pi - k_z L \tag{9}$$

where L is the length of the slit, m is integer order of resonance.

Figure 8 compares the phase of reflection calculated using the formulation above and the FDTD simulations with the theory presented in the last section. Equation 9 is the usual formula for the FP case. Here the difference is that Φ_r is modified for the lossy case following the theory outlined above. Good agreement is seen between the analytic theory and the comprehensive FDTD results, thus supporting the use of the unconjugated orthogonality formulation. Although a slight difference can be seen for shorter wavelengths and especially

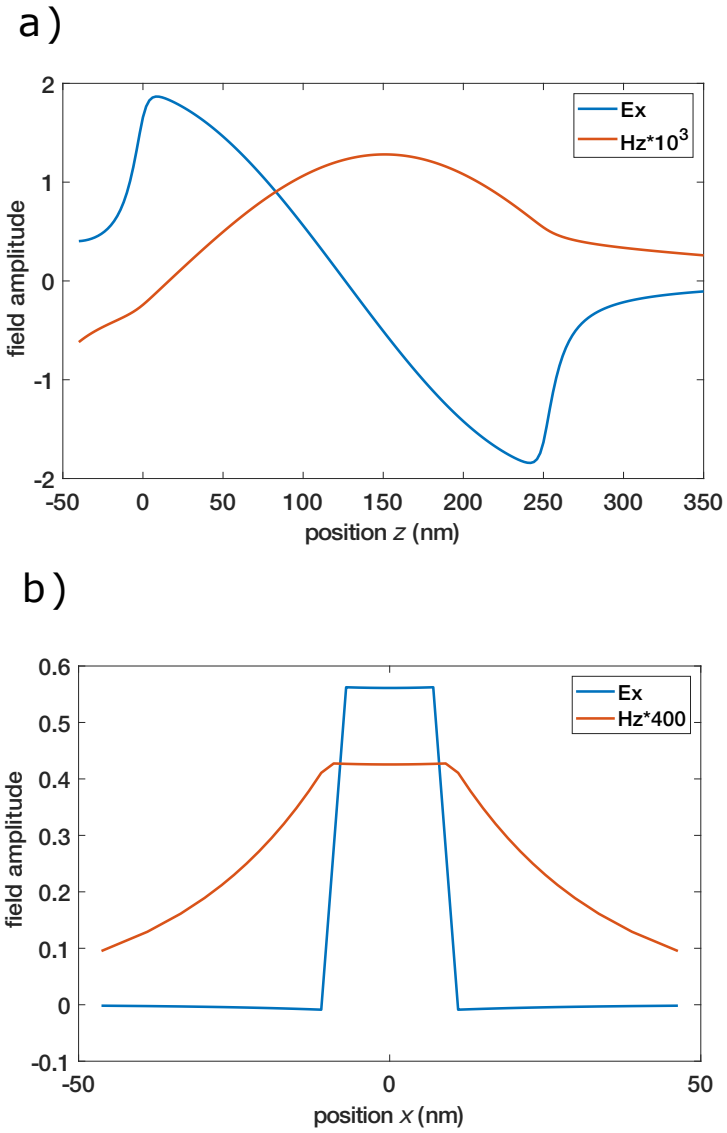

Fig. 6 Electric and magnetic fields inside the structure a) in the z direction (for $x = 0$. b) in the x direction (for $z = 150$ nm.

for the shortest slit width, comparing this Figure with Figure 4 shows that the unconjugated method results are close to the simulation results. The difference between our results and the simulation results comes from simulation accuracy and the approximation in the single mode matching theory.

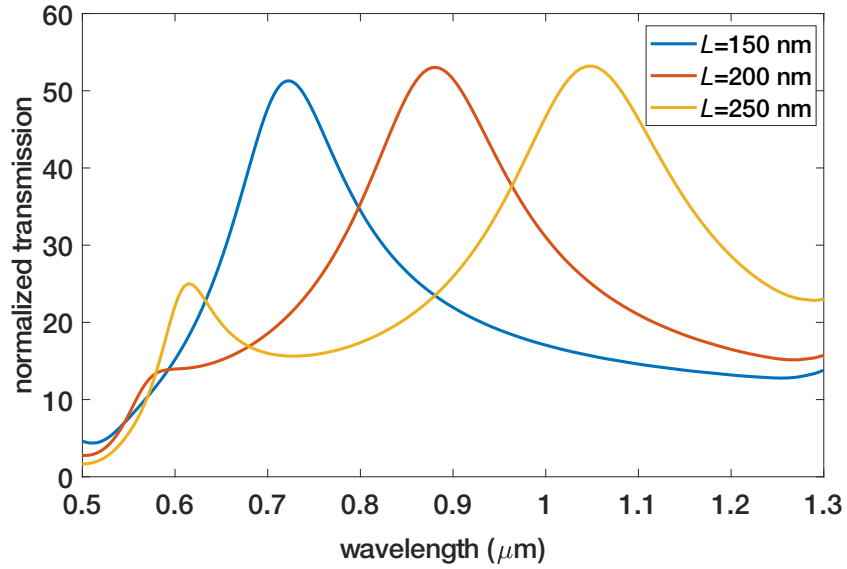

Fig. 7 Transmission through a 20 nm wide slit in an Au-air-Au structure as a function of wavelength. The transmission peak wavelength increases by increasing the slit length.

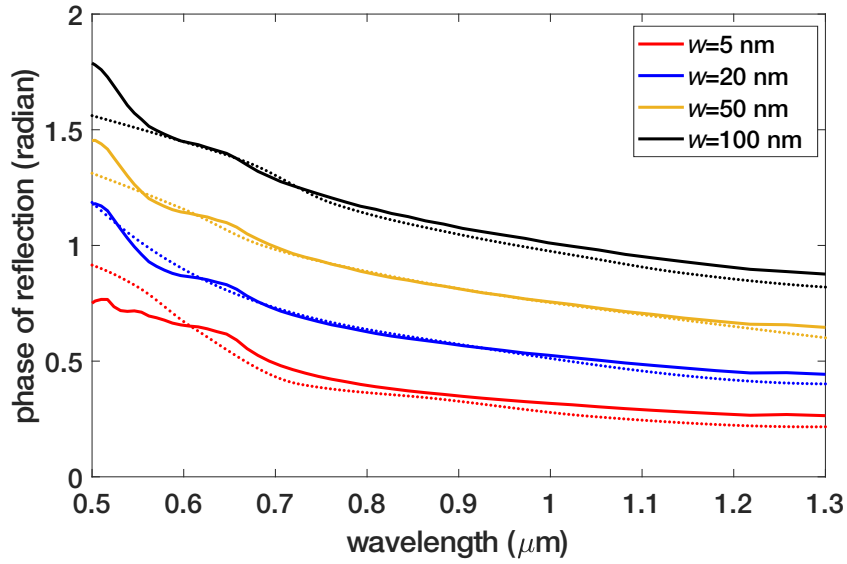

Fig. 8 Reflection phase using unconjugated method in comparison with FDTD simulations in an Au-air-Au structure. Solid lines show the results using unconjugated form of the orthogonality and dotted lines are from the simulations.

4 Comparison with experimental data

We compare the theory with a past experiment of narrow slits using a silica spacer layer [1]. A dielectric constant of $\epsilon_d = 2.1$ was used in Eq. 2 to match the experimental conditions.

Fig. 9 shows the experimental data of the MIM waveguides for different slit widths and lengths, digitized from [1]. The theoretical dispersion curves are shown for three different cases: the dashed line ignores the phase of reflection, the thick solid line is from the theory presented above and the dotted line is our FDTD simulation. Clearly, the phase of reflection plays an important role in determining the plasmonic resonances seen in experiment, and the simple theory presented above accurately accounts for this phase.

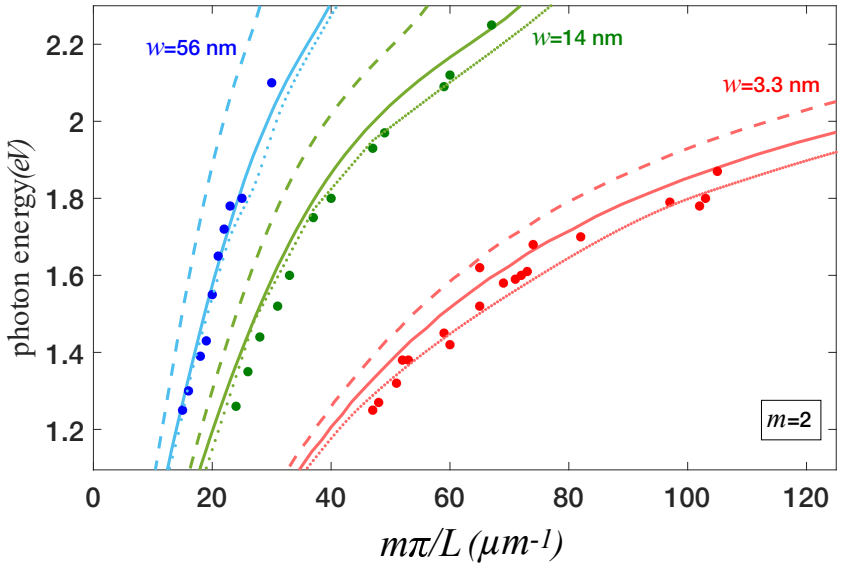

Fig. 9 Dispersion relation for an Au-Silica-Au structure. Solid lines: calculation of dispersion considering the effect of the reflection phase calculated using unconjugated form of the orthogonality relation. Dashed lines: calculation of dispersion ignoring the effect of the reflection phase as was done in the past analysis. Dotted lines: FDTD simulation. Discrete points: experimental results using the experimentally measured plasmonic resonances [1]. The theory presented above shows good agreement with both FDTD and experiment.

5 Conclusion

In conclusion, we have provided a theory for the phase of reflection from a plasmonic slit that incorporates the real loss of the metal using the unconjugated form of the orthogonality relation. The impact of the real loss on the reflection phase is significant. Thereby, the imaginary part of the permittivity impacts not only the quality factor, but also the plasmonic resonance wavelength. The results for the unconjugated form differ significantly from the conjugated form that was presented in past works. The theory presented here agrees well with full-field FDTD simulations and past experiments, showing promise for simple theoretical investigation of future plasmonic MIM structures.

Funding

The authors are funded by the Natural Sciences and Engineering Research Council Discovery Grant (RGPIN-2017-03830).

Conflicts of interest/Competing interests

The authors declare that they have no conflict of interest.

Availability of data and material (data transparency)

All relevant data is presented in the manuscript.

Code availability (software application or custom code)

Lumerical and Matlab code can be made available at reasonable request.

Authors' contributions

ZS performed all calculations. ZS and RG conceived of approach, developed theory, wrote manuscript.

Ethics approval

Not applicable.

Consent to participate

Not applicable.

Consent for publication

Not applicable.

References

1. H.T. Miyazaki, Y. Kurokawa, Phys. Rev. Lett. **96**(9), 097401 (2006)
2. K.J. Russell, T.L. Liu, S. Cui, E.L. Hu, Nat. Photon. **6**(7), 459 (2012)
3. J.K. Yang, C.S. Kee, J.W. Lee, Opt. Express **19**(21), 20199 (2011)
4. H. Choo, M.K. Kim, M. Staffaroni, T.J. Seok, J. Bokor, S. Cabrini, P.J. Schuck, M.C. Wu, E. Yablonovitch, Nat. Photon. **6**(12), 838 (2012)
5. X. Chen, H.R. Park, N.C. Lindquist, J. Shaver, M. Pelton, S.H. Oh, Sci. Rep. **4**(1), 1 (2014)
6. M. Seo, H. Park, S. Koo, D. Park, J. Kang, O. Suwal, S. Choi, P. Planken, G. Park, N. Park, H. Park, D. Kim, Nat. Photon. **3**(3), 152 (2009)
7. O.K. Suwal, J. Rhie, N. Kim, D.S. Kim, Sci. Rep. **7**, 45638 (2017)
8. Y.M. Bahk, S. Han, J. Rhie, J. Park, H. Jeon, N. Park, D.S. Kim, Phys. Rev. B **95**(7), 075424 (2017)
9. H.T. Miyazaki, Y. Kurokawa, Appl. Phys. Lett. **89**(21), 211126 (2006)
10. F. García-Vidal, E. Moreno, J. Porto, L. Martin-Moreno, Phys. Rev. Lett. **95**(10), 103901 (2005)
11. J.R. Suckling, A.P. Hibbins, M.J. Lockyear, T. Preist, J.R. Sambles, C.R. Lawrence, Phys. Rev. Lett. **92**(14), 147401 (2004)
12. J.S. White, G. Veronis, Z. Yu, E.S. Barnard, A. Chandran, S. Fan, M.L. Brongersma, Opt. Lett. **34**(5), 686 (2009)
13. T. Ishi, J. Fujikata, K. Makita, T. Baba, K. Ohashi, Japanese Journal of Applied Physics **44**(3L), L364 (2005)
14. S. Refki, S. Hayashi, A. Rahmouni, D.V. Nesterenko, Z. Sekkat, Plasmonics **11**(2), 433 (2016)
15. Z. Sekkat, S. Hayashi, D.V. Nesterenko, A. Rahmouni, S. Refki, H. Ishitobi, Y. Inouye, S. Kawata, Opt. Express **24**(18), 20080 (2016)
16. S. Hayashi, D. Nesterenko, A. Rahmouni, Z. Sekkat, Phys. Rev. B **95**(16), 165402 (2017)
17. K. Wen, L. Yan, W. Pan, B. Luo, Z. Guo, Y. Guo, Opt. Eng. **51**(10), 104601 (2012)
18. Y.C. Jun, K.C. Huang, M.L. Brongersma, Nat. Commun. **2**(1), 1 (2011)
19. P. Neutens, P. Van Dorpe, I. De Vlaminck, L. Lagae, G. Borghs, Nat. Photon. **3**(5), 283 (2009)
20. Y. Kurokawa, H.T. Miyazaki, Phys. Rev. B **75**(3), 035411 (2007)
21. N.C. Lindquist, P. Nagpal, K.M. McPeak, D.J. Norris, S.H. Oh, Rep. Prog. Phys. **75**(3), 036501 (2012)
22. Y. Takakura, Phys. Rev. Lett. **86**(24), 5601 (2001)
23. R. Gordon, Phys. Rev. B **73**(15), 153405 (2006)
24. F. Yang, J.R. Sambles, Phys. Rev. Lett **89**(6), 063901 (2002)
25. L. Novotny, Phys. Rev. Lett **98**(26), 266802 (2007)
26. J. Park, H. Kim, I.M. Lee, S. Kim, J. Jung, B. Lee, Opt. Express **16**(21), 16903 (2008)
27. H. Jamid, S. Al-Bader, IEEE Photon. Technol. Lett **7**(3), 321 (1995)
28. T. Leskova, N. Gapotchenko, Solid State Commun. **53**(4), 351 (1985)
29. T. Leskova, A. Maradudin, W. Zierau, Opt. Commun. **249**(1-3), 23 (2005)
30. A. Chandran, E.S. Barnard, J.S. White, M.L. Brongersma, Phys. Rev. B **85**(8), 085416 (2012)
31. W.P. Huang, J. Mu, Optics express **17**(21), 19134 (2009)
32. S.B. Hasan, R. Filter, A. Ahmed, R. Vogelgesang, R. Gordon, C. Rockstuhl, F. Lederer, Physical Review B **84**(19), 195405 (2011)